### Title
Analyzing the Intensities of K–Edge Transitions in X2 Molecules (X = F, Cl, Br) for Use in Ligand K–Edge X–ray Absorption Spectroscopy




### Journal
Inorganic Chemistry, 63(34)

### ISSN
0020-1669



### Authors
Branson, Jacob A
Smith, Patrick W
Arnold, John
et al.



### Publication Date
2024-08-26

### DOI
10.1021/acs.inorgchem.4c01666

Inorganic Chemistry



pubs.acs.org/IC
Communication

# Analyzing the Intensities of K-Edge Transitions in $X_2$ Molecules (X = F, Cl, Br) for Use in Ligand K-Edge X-ray Absorption Spectroscopy

Jacob A. Branson,* Patrick W. Smith, John Arnold, and Stefan G. Minasian

Cite This: *Inorg. Chem.* 2024, 63, 15557−15562
Read Online
ACCESS | Metrics & More | Article Recommendations

**ABSTRACT:** Ligand K-edge X-ray absorption spectroscopy (XAS) is regularly used to determine the ligand contribution to metal−ligand bonds. For quantitative studies, the pre-edge transition intensities must be referenced to an intensity standard, and pre-edge intensities obtained from different ligand atoms cannot be compared without standardization due to different cross sections at each absorption edge. In this work, the intensities of the 1s → $\sigma^*$ transitions in $F_2$, $Cl_2$, and $Br_2$ are analyzed for their use as references for ligand K-edge XAS. We show that the intensities of these transitions are equal to the intensities of the 1s → *n*p transitions in the unbound halogens. This finding is supported by a comparison between the normalized experimental intensities for the molecules and the calculated oscillator strengths for the atoms. These results highlight the potential for these molecules to be used as intensity standards in F, Cl, and Br K-edge XAS experiments.

The ligand orbital contribution to metal−ligand bonds is frequently evaluated by performing X-ray absorption spectroscopy (XAS) at the K-edge for ligand donor atoms: a technique that is collectively referred to as "ligand K-edge XAS". This technique probes transitions of localized ligand 1s electrons to primarily metal-based molecular orbitals (MOs). The transition intensity is weighted by the amount of ligand *p*-orbital character ($\lambda^2$) in the acceptor MO ($\Psi^*$) and by the intrinsic intensity of a ligand 1s → *n*p transition ($I_{1s\rightarrow np}$):[1,2]

$$I_{1s\rightarrow\Psi^*} = \frac{h}{N}\lambda^2 I_{1s\rightarrow np} \quad (1)$$

where *h* is the number of holes in the acceptor MO, *N* is the number of absorbing atoms, and *n* is the principal quantum number of the valence *p*-orbitals for a given ligand. By combining ligand K-edge XAS measurements with electronic structure calculations, Solomon and co-workers provided the first demonstrations of this approach to probe orbital mixing in transition metal complexes with M−Cl and M−S bonds.[2−7] Further studies have advanced this methodology for M−Cl[8−14] and M−S[15−21] bonds, and expanded the range of ligand chemistries to include systems incorporating M−P,[13,14,19,22−30] M−O,[31−37] M−N,[19,38−41] and M−C bonds.[42−47]

To interrogate bonding trends, previous ligand K-edge XAS studies varied the metal while holding the ligand constant. The opposite approach (varying the ligand) requires probing multiple ligand K-edges, which can pose technical challenges related to differences in sample preparation, X-ray spectrometer characteristics, and data reduction methods. In addition, intensities from different edges cannot be compared directly unless the value of $I_{1s\rightarrow np}$ is quantified at each edge. One approach to determine $I_{1s\rightarrow np}$ is to measure the ligand K-edge spectra of a compound with known $\lambda^2$ and use eq 1 to solve for $I_{1s\rightarrow np}$. For $D_{2d}$-$CuCl_4^{2-}$, $\lambda^2$ was determined using electron paramagnetic resonance (EPR) spectroscopy and later refined by comparison studies to $D_{4h}$-$CuCl_4^{2-}$ using EPR, Cu K-edge XAS, and Cl K-edge XAS.[48−52] This $\lambda^2$ was then used in tandem with the Cl K-edge XAS data to determine a value for $I_{Cl\ 1s\rightarrow Cl\ 3p}$.[2]

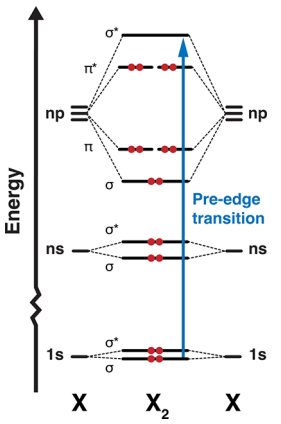


**Figure 1.** Qualitative MO diagram for dihalogen molecules. Electron occupancy is shown by red circles. The pre-edge transition studied here is represented by a blue arrow.

We began examining the dihalogen molecules ($F_2$, $Cl_2$, and $Br_2$) to understand how $I_{1s\rightarrow np}$ changes for F, Cl, and Br. For these homodiatomic molecules, each halogen atom contributes exactly half to the resulting MOs, $\lambda^2 = 0.5$ (Figure 1). The K-edge spectra of gaseous $F_2$, $Cl_2$, and $Br_2$ have been reported

Received: April 23, 2024
Revised: July 21, 2024
Accepted: July 31, 2024
Published: August 7, 2024

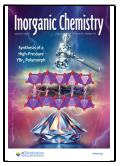





https://doi.org/10.1021/acs.inorgchem.4c01666
*Inorg. Chem.* 2024, 63, 15557−15562

and exhibit intense transitions to the antibonding $\sigma^*$ orbitals.[53−55] While the K-edge spectrum of $I_2$ has also been reported, the intensity of the 1s → $\sigma^*$ transition could not be quantified with high confidence owing to the much larger lifetime broadening.[55]

The results of our normalization and curve fitting for the previously reported[53−55] K-edge spectra of $F_2$, $Cl_2$, and $Br_2$ are shown in Figure 2. The spectrum for $F_2$ was collected via

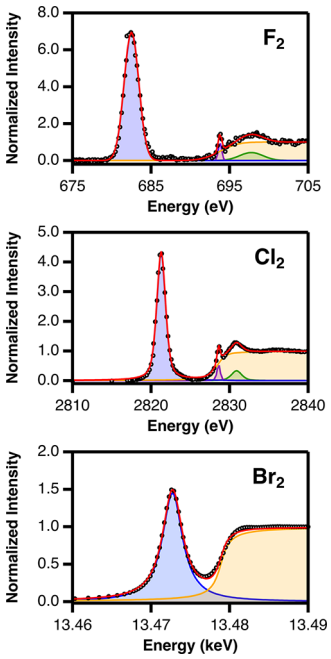


**Figure 2.** K-edge XAS spectra for $F_2$, $Cl_2$, and $Br_2$. Experimental data points (circles) are fit using pseudo-Voigt functions. The intense, lowest energy feature (blue) is assigned to the 1s → $\sigma^*$ transition. Higher energy features (purple and green) are associated with Rydberg transitions. The edge-step (orange) corresponds to the rising edge region. Experimental data were digitized from publications for $F_2$ (ref. 53) and $Cl_2$ (ref. 54), and obtained from the author of ref. 55 for $Br_2$.

electron energy-loss spectroscopy (EELS) while the spectra for $Cl_2$ and $Br_2$ were collected with synchrotron XAS in transmission mode. Data reduction and fitting were performed as previously described,[4,9,32] and the fit parameters for the $\sigma^*$ pre-edge transitions are presented in Table 1. The Lorentzian component ($\eta$) of the pseudo-Voigt functions was increased from 0% for F, to 50% for Cl, and 100% for Br to account for increased core-hole broadening. These $\eta$ were chosen as values

**Table 1. Fit Parameters for the 1s → $\sigma^*$ Transition in the Normalized K-Edge Spectra of Dihalogens**

| | peak energy (eV) | $\eta$ | height[c] | fwhm[c] | intensity[d] |
|---|---|---|---|---|---|
| $F_2$[a] | 682.5 | 0 | 6.97(5) | 2.20(2) | 16.3(8) |
| $Cl_2$[a] | 2821.3 | 0.5 | 4.33(4) | 1.33(2) | 7.6(4) |
| $Br_2$[b] | 13472.7 | 1 | 1.45(1) | 3.09(4) | 7.1(4) |

[a]Experimental spectra were digitized from published data sets for $F_2$ (ref 53) and $Cl_2$ (ref 54). [b]The spectrum of $Br_2$ (ref 55) was provided by the original author. [c]The error in the peak height and width are their standard deviations from the curve fit. [d]The estimated error in the integrated intensity (5%) accounts for the error introduced from data reduction, based on previous work.[4]

that well model experimental data and were constrained to reduce the number of free parameters in the fit. Based on previous work, the error in integrated intensities from background subtraction, normalization, and fitting is estimated to be 5%.[4]

The intensity of the 1s → $\sigma^*$ transition is described in terms of the dipole strength, $D_0$:

$$I_{1s\rightarrow\sigma^*} = kD_0 = \frac{k}{3|G|}\sum_{\alpha\beta\gamma}|\langle G_\alpha|\hat{r}_\beta|E_\gamma\rangle|^2 \quad (2)$$

where $G$ and $E$ are the many-electron ground and excited states, $|G|$ is the degeneracy of the ground state, $\hat{r}$ is the dipole operator, and $k$ is a constant scaling the dipole strength to experimental intensity. The indices $\alpha$, $\beta$, and $\gamma$ sum over the components of the ground state, dipole operator, and excited state. The constant $^1/_3$ derives from transforming $D_0$ from a space-fixed coordinate system into orientationally averaged, molecule-fixed operators.[56] The following derivation is similar to that of Shadle et al.,[2] omitting the reliance on bond length in accordance with a study by Neese et al. showing that the transition dipoles for K-edge excitations are localized on the absorbing atoms.[1]

For the 1s → $\sigma^*$ transition in a $D_{\infty h}$-$X_2$ molecule, the ground state, dipole operator, and excited state transform as $\sum_g^+$, $\sum_u^+$, and $\sum_u^+$, respectively. Because these irreducible representations are singly degenerate, the summation over their components may be omitted and $|G| = 1$, simplifying eq 2 to

$$I_{1s\rightarrow\sigma^*} = \frac{k}{3}|\langle\Sigma_g^+|\Sigma_u^+|\Sigma_u^+\rangle|^2 \quad (3)$$

Equation 3 contains many-electron states and must be related to one-electron states to define the intensity in terms of MO coefficients. This transformation begins by using eq 20.2.10 in Piepho and Schatz,[56] resulting in

$$I_{1s\rightarrow\sigma^*} = \frac{2k}{3}\langle\sigma_g^+||\sigma_u^+||\sigma_u^+\rangle^2 \quad (4)$$

where the magnitude of the many-electron matrix element has been replaced by a reduced matrix element.

To relate eq 4 to MO coefficients, a one-electron transition dipole matrix element between the donor ($\sigma_g^+$) and acceptor ($\sigma_u^+$) orbitals must be defined. Then, using Piepho and Schatz eq 10.2.2,[56] it is equated to a reduced matrix element.

$$\langle\sigma_g^+|\hat{r}|\sigma_u^+\rangle = \langle\sigma_g^+||\sigma_u^+||\sigma_u^+\rangle \quad (5)$$

This one-electron matrix element is equated to MO coefficients by substituting wave functions for the donor and acceptor orbitals from the linear combination of atomic orbitals approximation:

$$\langle\sigma_g^+|\hat{r}|\sigma_u^+\rangle = \langle\frac{1}{\sqrt{2}}(1s_1 + 1s_2)|\hat{r}_z|\frac{1}{\sqrt{2}}(np_{z,1} + np_{z,2})\rangle \quad (6)$$

where the subscripts on the atomic orbitals are atomic indices. Only the $z$ component of the dipole operator is considered because the acceptor $p$-orbitals lie only along that axis. Instead of the local coordinate system often used to define MOs, the acceptor $\sigma^*$ orbital is given in terms of a global coordinate system, in which the antibonding wave function is the additive combination of atomic orbitals (Figure 3). Furthermore, we have neglected overlap ($S_{12}$) in normalizing the acceptor wave function since ligand K-edge XAS measures the acceptor


https://doi.org/10.1021/acs.inorgchem.4c01666
Inorg. Chem. 2024, 63, 15557−15562

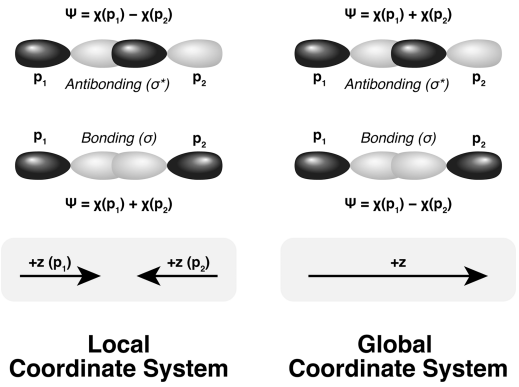


**Figure 3.** Visualization of transforming from a local coordinate system to a global coordinate system.

orbital population (which accounts for the overlap region) rather than orbital mixing coefficient.

This matrix element is evaluated by expansion into multiple matrix elements while neglecting two-center integrals.

$$\langle \sigma_g^+ | \hat{r} | \sigma_u^+ \rangle = \frac{1}{2}[\langle 1s_1 | \hat{r}_z | np_{z,1} \rangle + \langle 1s_2 | \hat{r}_z | np_{z,2} \rangle] \quad (7)$$

Because the terms on the right-hand side are equal matrix elements of $\hat{r}_z$, they are summed and the atomic indices dropped.

$$\langle \sigma_g^+ | \hat{r} | \sigma_u^+ \rangle = \langle 1s | \hat{r}_z | np_z \rangle \quad (8)$$

When eqs 5 and 8 are combined, the reduced matrix element is equal to the atomic one-electron matrix element.

$$\langle \sigma_g^+ || \sigma_u^+ || \sigma_u^+ \rangle = \langle 1s | \hat{r}_z | np_z \rangle \quad (9)$$

Then, when eqs 4 and 9 are combined and recalling that $|\langle 1s|\hat{r}_x|np_x\rangle|^2 = |\langle 1s|\hat{r}_y|np_y\rangle|^2 = |\langle 1s|\hat{r}_z|np_z\rangle|^2 = |\langle 1s|\hat{r}|np\rangle|^2$ for an atom, the ligand K-edge XAS intensity in terms of atomic orbitals is

$$I_{1s\rightarrow\sigma^*} = \frac{2k}{3} |\langle 1s|\hat{r}|np\rangle|^2 \quad (10)$$

To account for the per-atom normalization of the experimental data, the right side of eq 10 must be divided by $N$ (2 for $X_2$), producing the equation for the normalized intensity of the 1s → σ* transition in $X_2$.

$$I_{1s\rightarrow\sigma^*} = \frac{k}{3} |\langle 1s|\hat{r}|np\rangle|^2 \quad (11)$$

Finally, to directly relate this equation to the intrinsic intensity of the absorbing atoms, eq 2 is applied to the 1s → $n$p transition of an unbound halogen atom.

$$I_{1s\rightarrow np} = kD_0 = \frac{k}{3|P|} \sum_i |\langle 1s|\hat{r}_i|np_i\rangle|^2 = \frac{k}{9} \sum_i |\langle 1s|\hat{r}_i|np_i\rangle|^2 = \frac{k}{3} |\langle 1s|\hat{r}|np\rangle|^2 \quad (12)$$

where $i = x$, $y$, and $z$ Cartesian components. When eqs 11 and 12 are combined, the final relationship between dihalogen $I_{1s\rightarrow\sigma^*}$ and halogen $I_{1s\rightarrow np}$ is simply,

$$I_{1s\rightarrow\sigma^*} = I_{1s\rightarrow np} \quad (13)$$

Thus, the 1s → $n$p transition intensities for F, Cl, and Br are equal to the corresponding 1s → σ* transition intensities in $F_2$, $Cl_2$, and $Br_2$.

To verify this relationship, the oscillator strengths ($f_{1s,np}$) of the 1s → $n$p transitions in the F, Cl, and Br atoms were calculated using Cowan's atomic structure codes[57] within the *Missing 1.11* user interface.[58] The default value for Slater integral rescaling was used, 0.8, and the spin−orbit coupling was not rescaled. Table 2 compares the resulting $f_{1s,np}$ values to the experimental intensities, which were normalized to the K-edge absorption cross section of the absorbing atom. The calculations show that $f_{1s,np}$ decreases by a factor of ∼10 on moving from F to Cl, followed by an additional decrease by a factor of ∼2 on moving from Cl to Br. A comparable decrease is observed experimentally, beginning with a 10-fold decrease in intensity moving from $F_2$ to $Cl_2$, followed by a ∼6-fold decrease moving from $Cl_2$ to $Br_2$. This agreement between the calculated $f_{1s,np}$ and normalized intensities supports using this methodology for determining atomic parameters from molecular units.

**Table 2. Comparison between Calculated Oscillator Strengths for the Halogen 1s → $n$p Transition and the $X_2$ Pre-edge Intensities Normalized to the K-Edge Absorption Cross Section**

| | K-edge absorption cross section ($\times 10^4$ cm$^2$ mol$^{-1}$)[59] | normalized pre-edge intensity ($\times 10^4$ eV cm$^2$ mol$^{-1}$)[a] | $f_{1s,np} \times 1000$ |
|---|---|---|---|
| $F_2$ | 23.02 | 376(19) | 261.49 |
| $Cl_2$ | 5.42 | 41(2) | 33.69 |
| $Br_2$ | 1.04 | 7.3(4) | 17.8 |

[a]Obtained by multiplication of the transition intensities in Table 1 by the K-edge absorption cross sections.

With these $I_{1s\rightarrow np}$ supported by atomic structure calculations, we will consider their use in quantitative ligand K-edge XAS. When comparing these rigorously covalent molecules with metal−halide bonds, it is important to consider that the intrinsic intensity is dependent on the charge of the absorbing atom. Thus, some error is introduced when analyzing metal−halide complexes (which contain anionic halogens) using these covalent standards. However, the change in intensity as a function of charge density has been calculated to be very low (<5%).[2] Additionally, there is statistical equivalence between the $I_{Cl\ 1s\rightarrow Cl\ 3p}$ value reported here, 7.6(4), from $Cl_2$ and that determined from $D_{2d}$-$CuCl_4^{2-}$, 7.0(2).[2,7] Further factors which can effect data quantification include differences in sample preparation, data acquisition, and data reduction.[4,31,34,37] Hence, while the agreement between the $I_{Cl\ 1s\rightarrow Cl\ 3p}$ values for $Cl_2$ and $D_{2d}$-$CuCl_4^{2-}$ is encouraging for the use of $Cl_2$ and as an intensity standard, additional work is needed to provide experimental validation for the use of $F_2$ and $Br_2$.

This work shows that the 1s → σ* transition in the K-edge spectra of $F_2$, $Cl_2$, and $Br_2$ may be used to calibrate pre-edge intensities in ligand K-edge XAS. These findings are supported by comparison between the experimental intensities and the calculated oscillator strengths for the unbound atoms. Furthermore, the use of these $I_{1s\rightarrow np}$ in ligand K-edge XAS analysis is supported by the agreement between the $I_{1s\rightarrow 3p}$ for Cl determined here and in previous studies. Additional work to validate these findings with other spectroscopic probes of metal−ligand orbital mixing is ongoing.



https://doi.org/10.1021/acs.inorgchem.4c01666
Inorg. Chem. 2024, 63, 15557−15562

## AUTHOR INFORMATION


### Corresponding Author

**Jacob A. Branson** − *Department of Chemistry, University of California, Berkeley, Berkeley, California 94720, United States; Chemical Sciences Division, Lawrence Berkeley National Laboratory (LBNL), Berkeley, California 94720, United States;* orcid.org/0000-0002-3523-0303; Email: jacob.branson@berkeley.edu

### Authors

**Patrick W. Smith** − *Chemical Sciences Division, Lawrence Berkeley National Laboratory (LBNL), Berkeley, California 94720, United States;* orcid.org/0000-0001-5575-4895

**John Arnold** − *Department of Chemistry, University of California, Berkeley, Berkeley, California 94720, United States; Chemical Sciences Division, Lawrence Berkeley National Laboratory (LBNL), Berkeley, California 94720, United States;* orcid.org/0000-0001-9671-227X

**Stefan G. Minasian** − *Chemical Sciences Division, Lawrence Berkeley National Laboratory (LBNL), Berkeley, California 94720, United States;* orcid.org/0000-0003-1346-7497

Complete contact information is available at: https://pubs.acs.org/10.1021/acs.inorgchem.4c01666


### Notes

The authors declare no competing financial interest.

## ACKNOWLEDGMENTS

The authors are grateful to Adriano Filipponi for providing the raw data file for the Br K-edge spectrum of $Br_2$. This work was supported by the Director, Office of Science, Office of Basic Energy Sciences, Division of Chemical Sciences, Geosciences, and Biosciences Heavy Element Chemistry Program of the U.S. Department of Energy (DOE) at LBNL under Contract DE-AC02-05CH11231. J.A.B. received funding from the U.S. DOE through the Office of Nuclear Energy, Integrated University Program Graduate Fellowship.

## REFERENCES


(1) Neese, F.; Hedman, B.; Hodgson, K. O.; Solomon, E. I. Relationship between the Dipole Strength of Ligand Pre-Edge Transitions and Metal−Ligand Covalency. *Inorg. Chem.* **1999**, *38* (21), 4854−4860.

(2) Shadle, S. E.; Hedman, B.; Hodgson, K. O.; Solomon, E. I. Ligand K-Edge X-ray Absorption Spectroscopic Studies: Metal-Ligand Covalency in a Series of Transition Metal Tetrachlorides. *J. Am. Chem. Soc.* **1995**, *117* (8), 2259−2272.

(3) Shadle, S. E.; Hedman, B.; Hodgson, K. O.; Solomon, E. I. Ligand K-Edge X-Ray Absorption Spectroscopy as a Probe of Ligand-Metal Bonding: Charge Donation and Covalency in Copper-Chloride Systems. *Inorg. Chem.* **1994**, *33* (19), 4235−4244.

(4) Solomon, E. I.; Hedman, B.; Hodgson, K. O.; Dey, A.; Szilagyi, R. K. Ligand K-Edge X-Ray Absorption Spectroscopy: Covalency of Ligand−Metal Bonds. *Coord. Chem. Rev.* **2005**, *249* (1−2), 97−129.

(5) Randall, D. W.; George, S. D.; Hedman, B.; Hodgson, K. O.; Fujisawa, K.; Solomon, E. I. Spectroscopic and Electronic Structural Studies of Blue Copper Model Complexes. 1. Perturbation of the Thiolate−Cu Bond. *J. Am. Chem. Soc.* **2000**, *122* (47), 11620−11631.

(6) Randall, D. W.; George, S. D.; Holland, P. L.; Hedman, B.; Hodgson, K. O.; Tolman, W. B.; Solomon, E. I. Spectroscopic and Electronic Structural Studies of Blue Copper Model Complexes. 2. Comparison of Three- and Four-Coordinate Cu(II)−Thiolate Complexes and Fungal Laccase. *J. Am. Chem. Soc.* **2000**, *122* (47), 11632−11648.

(7) Glaser, T.; Hedman, B.; Hodgson, K. O.; Solomon, E. I. Ligand K-Edge X-Ray Absorption Spectroscopy: A Direct Probe of Ligand−Metal Covalency. *Acc. Chem. Res.* **2000**, *33* (12), 859−868.

(8) DeBeer George, S.; Brant, P.; Solomon, E. I. Metal and Ligand K-Edge XAS of Organotitanium Complexes: Metal 4p and 3d Contributions to Pre-Edge Intensity and Their Contributions to Bonding. *J. Am. Chem. Soc.* **2005**, *127* (2), 667−674.

(9) Minasian, S. G.; Keith, J. M.; Batista, E. R.; Boland, K. S.; Clark, D. L.; Conradson, S. D.; Kozimor, S. A.; Martin, R. L.; Schwarz, D. E.; Shuh, D. K.; Wagner, G. L.; Wilkerson, M. P.; Wolfsberg, L. E.; Yang, P. Determining Relative f and d Orbital Contributions to M−Cl Covalency in $MCl_6^{2-}$ (M = Ti, Zr, Hf, U) and $UOCl_5^-$ Using Cl K-Edge X-Ray Absorption Spectroscopy and Time-Dependent Density Functional Theory. *J. Am. Chem. Soc.* **2012**, *134* (12), 5586−5597.

(10) Cross, J. N.; Su, J.; Batista, E. R.; Cary, S. K.; Evans, W. J.; Kozimor, S. A.; Mocko, V.; Scott, B. L.; Stein, B. W.; Windorff, C. J.; Yang, P. Covalency in Americium(III) Hexachloride. *J. Am. Chem. Soc.* **2017**, *139* (25), 8667−8677.

(11) Kozimor, S. A.; Yang, P.; Batista, E. R.; Boland, K. S.; Burns, C. J.; Christensen, C. N.; Clark, D. L.; Conradson, S. D.; Hay, P. J.; Lezama, J. S.; Martin, R. L.; Schwarz, D. E.; Wilkerson, M. P.; Wolfsberg, L. E. Covalency Trends in Group IV Metallocene Dichlorides. Chlorine K-Edge X-Ray Absorption Spectroscopy and Time Dependent-Density Functional Theory. *Inorg. Chem.* **2008**, *47* (12), 5365−5371.

(12) Kozimor, S. A.; Yang, P.; Batista, E. R.; Boland, K. S.; Burns, C. J.; Clark, D. L.; Conradson, S. D.; Martin, R. L.; Wilkerson, M. P.; Wolfsberg, L. E. Trends in Covalency for D- and f-Element Metallocene Dichlorides Identified Using Chlorine K-Edge X-Ray Absorption Spectroscopy and Time-Dependent Density Functional Theory. *J. Am. Chem. Soc.* **2009**, *131* (34), 12125−12136.

(13) Mossin, S.; Tran, B. L.; Adhikari, D.; Pink, M.; Heinemann, F. W.; Sutter, J.; Szilagyi, R. K.; Meyer, K.; Mindiola, D. J. A Mononuclear Fe(III) Single Molecule Magnet with a 3/2↔5/2 Spin Crossover. *J. Am. Chem. Soc.* **2012**, *134* (33), 13651−13661.

(14) Soma, S.; Van Stappen, C.; Kiss, M.; Szilagyi, R. K.; Lehnert, N.; Fujisawa, K. Distorted Tetrahedral Nickel-Nitrosyl Complexes: Spectroscopic Characterization and Electronic Structure. *JBIC J. Biol. Inorg. Chem.* **2016**, *21* (5), 757−775.

(15) Sarangi, R.; DeBeer George, S.; Rudd, D. J.; Szilagyi, R. K.; Ribas, X.; Rovira, C.; Almeida, M.; Hodgson, K. O.; Hedman, B.; Solomon, E. I. Sulfur K-Edge X-Ray Absorption Spectroscopy as a Probe of Ligand−Metal Bond Covalency: Metal vs Ligand Oxidation in Copper and Nickel Dithiolene Complexes. *J. Am. Chem. Soc.* **2007**, *129* (8), 2316−2326.

(16) Ha, Y.; Arnold, A. R.; Nuñez, N. N.; Bartels, P. L.; Zhou, A.; David, S. S.; Barton, J. K.; Hedman, B.; Hodgson, K. O.; Solomon, E. I. Sulfur K-Edge XAS Studies of the Effect of DNA Binding on the [Fe4S4] Site in EndoIII and MutY. *J. Am. Chem. Soc.* **2017**, *139* (33), 11434−11442.

(17) Olson, A. C.; Keith, J. M.; Batista, E. R.; Boland, K. S.; Daly, S. R.; Kozimor, S. A.; MacInnes, M. M.; Martin, R. L.; Scott, B. L. Using Solution- and Solid-State S K-Edge X-Ray Absorption Spectroscopy with Density Functional Theory to Evaluate M−S Bonding for $MS4^{2-}$ (M = Cr, Mo, W) Dianions. *Dalton Trans.* **2014**, *43* (46), 17283−17295.

(18) Queen, M. S.; Towey, B. D.; Murray, K. A.; Veldkamp, B. S.; Byker, H. J.; Szilagyi, R. K. Electronic Structure of [Ni(II)S4] Complexes from S K-Edge X-Ray Absorption Spectroscopy. *Coord. Chem. Rev.* **2013**, *257* (2), 564−578.

(19) Shearer, J.; Callan, P. E.; Masitas, C. A.; Grapperhaus, C. A. Influence of Sequential Thiolate Oxidation on a Nitrile Hydratase Mimic Probed by Multiedge X-Ray Absorption Spectroscopy. *Inorg. Chem.* **2012**, *51* (11), 6032−6045.

(20) Szilagyi, R. K.; Lim, B. S.; Glaser, T.; Holm, R. H.; Hedman, B.; Hodgson, K. O.; Solomon, E. I. Description of the Ground State Wave Functions of Ni Dithiolenes Using Sulfur K-Edge X-Ray Absorption Spectroscopy. *J. Am. Chem. Soc.* **2003**, *125* (30), 9158−9169.

(21) Szilagyi, R. K.; Bryngelson, P. A.; Maroney, M. J.; Hedman, B.; Hodgson, K. O.; Solomon, E. I. S K-Edge X-Ray Absorption Spectroscopic Investigation of the Ni-Containing Superoxide Dismutase Active Site: New Structural Insight into the Mechanism. *J. Am. Chem. Soc.* **2004**, *126* (10), 3018−3019.
(22) Harkins, S. B.; Mankad, N. P.; Miller, A. J. M.; Szilagyi, R. K.; Peters, J. C. Probing the Electronic Structures of [Cu2($\mu$-XR2)]N+ Diamond Cores as a Function of the Bridging X Atom (X = N or P) and Charge (n = 0, 1, 2). *J. Am. Chem. Soc.* **2008**, *130* (11), 3478−3485.
(23) Lee, K.; Wei, H.; Blake, A. V.; Donahue, C. M.; Keith, J. M.; Daly, S. R. Ligand K-Edge XAS, DFT, and TDDFT Analysis of Pincer Linker Variations in Rh(I) PNP Complexes: Reactivity Insights from Electronic Structure. *Dalton Trans.* **2016**, *45* (24), 9774−9785.
(24) Mankad, N. P.; Antholine, W. E.; Szilagyi, R. K.; Peters, J. C. Three-Coordinate Copper(I) Amido and Aminyl Radical Complexes. *J. Am. Chem. Soc.* **2009**, *131* (11), 3878−3880.
(25) Hu, Y.; Maclennan, A.; Sham, T. K. Electronic Structure and Optical Luminescence Studies of Ru Based OLED Compounds. *J. Lumin.* **2015**, *166*, 143−147.
(26) Adhikari, D.; Mossin, S.; Basuli, F.; Huffman, J. C.; Szilagyi, R. K.; Meyer, K.; Mindiola, D. J. Structural, Spectroscopic, and Theoretical Elucidation of a Redox-Active Pincer-Type Ancillary Applied in Catalysis. *J. Am. Chem. Soc.* **2008**, *130* (11), 3676−3682.
(27) Donahue, C. M.; Daly, S. R. Ligand K-Edge XAS Studies of Metal-Phosphorus Bonds: Applications, Limitations, and Opportunities. *Comments Inorg. Chem.* **2018**, *38* (2), 54−78.
(28) Donahue, C. M.; McCollom, S. P.; Forrest, C. M.; Blake, A. V.; Bellott, B. J.; Keith, J. M.; Daly, S. R. Impact of Coordination Geometry, Bite Angle, and Trans Influence on Metal−Ligand Covalency in Phenyl-Substituted Phosphine Complexes of Ni and Pd. *Inorg. Chem.* **2015**, *54* (12), 5646−5659.
(29) Kim, P.-S. G.; Hu, Y. F.; Puddephatt, R. J.; Sham, T. K. X-Ray Excited Optical Luminescence Studies of PPh3AuCl: Site-Specificity at the C and P K-Edges and the Au $M_{5,4}$-Edges. *Phys. Scr.* **2005**, *2005* (T115), 545.
(30) Kim, P.-S. G.; Hu, Y.; Brandys, M.-C.; Burchell, T. J.; Puddephatt, R. J.; Sham, T. K. X-Ray-Excited Optical Luminescence (XEOL) and X-Ray Absorption Fine Structures (XAFS) Studies of Gold(I) Complexes with Diphosphine and Bipyridine Ligands. *Inorg. Chem.* **2007**, *46* (3), 949−957.
(31) Bradley, J. A.; Yang, P.; Batista, E. R.; Boland, K. S.; Burns, C. J.; Clark, D. L.; Conradson, S. D.; Kozimor, S. A.; Martin, R. L.; Seidler, G. T.; Scott, B. L.; Shuh, D. K.; Tyliszczak, T.; Wilkerson, M. P.; Wolfsberg, L. E. Experimental and Theoretical Comparison of the O K-Edge Nonresonant Inelastic X-Ray Scattering and X-Ray Absorption Spectra of $NaReO_4$. *J. Am. Chem. Soc.* **2010**, *132* (39), 13914−13921.
(32) Minasian, S. G.; Batista, E. R.; Booth, C. H.; Clark, D. L.; Keith, J. M.; Kozimor, S. A.; Lukens, W. W.; Martin, R. L.; Shuh, D. K.; Stieber, S. C. E.; Tyliszczak, T.; Wen, X. Quantitative Evidence for Lanthanide-Oxygen Orbital Mixing in $CeO_2$, $PrO_2$, and $TbO_2$. *J. Am. Chem. Soc.* **2017**, *139* (49), 18052−18064.
(33) Altman, A. B.; Pacold, J. I.; Wang, J.; Lukens, W. W.; Minasian, S. G. Evidence for 5d-$\sigma$ and 5d-$\pi$ Covalency in Lanthanide Sesquioxides from Oxygen K-Edge X-Ray Absorption Spectroscopy. *Dalton Trans.* **2016**, *45* (24), 9948−9961.
(34) Minasian, S. G.; Keith, J. M.; Batista, E. R.; Boland, K. S.; Bradley, J. A.; Daly, S. R.; Kozimor, S. A.; Lukens, W. W.; Martin, R. L.; Nordlund, D.; Seidler, G. T.; Shuh, D. K.; Sokaras, D.; Tyliszczak, T.; Wagner, G. L.; Weng, T.-C.; Yang, P. Covalency in Metal−Oxygen Multiple Bonds Evaluated Using Oxygen K-Edge Spectroscopy and Electronic Structure Theory. *J. Am. Chem. Soc.* **2013**, *135* (5), 1864−1871.
(35) de Groot, F. M. F.; Faber, J.; Michiels, J. J. M.; Czyżyk, M. T.; Abbate, M.; Fuggle, J. C. Oxygen 1s X-Ray Absorption of Tetravalent Titanium Oxides: A Comparison with Single-Particle Calculations. *Phys. Rev. B* **1993**, *48* (4), 2074−2080.
(36) de Groot, F. M. F.; Grioni, M.; Fuggle, J. C.; Ghijsen, J.; Sawatzky, G. A.; Petersen, H. Oxygen 1s X-Ray-Absorption Edges of Transition-Metal Oxides. *Phys. Rev. B* **1989**, *40* (8), 5715−5723.
(37) Frati, F.; Hunault, M. O. J. Y.; de Groot, F. M. F. Oxygen K-Edge X-Ray Absorption Spectra. *Chem. Rev.* **2020**, *120* (9), 4056−4110.
(38) Lukens, J. T.; DiMucci, I. M.; Kurogi, T.; Mindiola, D. J.; Lancaster, K. M. Scrutinizing Metal−Ligand Covalency and Redox Non-Innocence *via* Nitrogen K-Edge X-Ray Absorption Spectroscopy. *Chem. Sci.* **2019**, *10* (19), 5044−5055.
(39) Dumas, T.; Guillaumont, D.; Fillaux, C.; Scheinost, A.; Moisy, P.; Petit, S.; Shuh, D. K.; Tyliszczak, T.; Auwer, C. D. The Nature of Chemical Bonding in Actinide and Lanthanide Ferrocyanides Determined by X-Ray Absorption Spectroscopy and Density Functional Theory. *Phys. Chem. Chem. Phys.* **2016**, *18* (4), 2887−2895.
(40) Pemmaraju, C. D.; Copping, R.; Wang, S.; Janousch, M.; Teat, S. J.; Tyliszczak, T.; Canning, A.; Shuh, D. K.; Prendergast, D. Bonding and Charge Transfer in Nitrogen-Donor Uranyl Complexes: Insights from NEXAFS Spectra. *Inorg. Chem.* **2014**, *53* (21), 11415−11425.
(41) Carsch, K. M.; DiMucci, I. M.; Iovan, D. A.; Li, A.; Zheng, S.-L.; Titus, C. J.; Lee, S. J.; Irwin, K. D.; Nordlund, D.; Lancaster, K. M.; Betley, T. A. Synthesis of a Copper-Supported Triplet Nitrene Complex Pertinent to Copper-Catalyzed Amination. *Science* **2019**, *365* (6458), 1138−1143.
(42) Minasian, S. G.; Keith, J. M.; Batista, E. R.; Boland, K. S.; Clark, D. L.; Kozimor, S. A.; Martin, R. L.; Shuh, D. K.; Tyliszczak, T. New Evidence for 5f Covalency in Actinocenes Determined from Carbon K-Edge XAS and Electronic Structure Theory. *Chem. Sci.* **2014**, *5* (1), 351−359.
(43) Minasian, S. G.; Keith, J. M.; Batista, E. R.; Boland, K. S.; Kozimor, S. A.; Martin, R. L.; Shuh, D. K.; Tyliszczak, T.; Vernon, L. J. Carbon K-Edge X-Ray Absorption Spectroscopy and Time-Dependent Density Functional Theory Examination of Metal−Carbon Bonding in Metallocene Dichlorides. *J. Am. Chem. Soc.* **2013**, *135* (39), 14731−14740.
(44) Smiles, D. E.; Batista, E. R.; Booth, C. H.; Clark, D. L.; Keith, J. M.; Kozimor, S. A.; Martin, R. L.; Minasian, S. G.; Shuh, D. K.; Stieber, S. C. E.; Tyliszczak, T. The Duality of Electron Localization and Covalency in Lanthanide and Actinide Metallocenes. *Chem. Sci.* **2020**, *11* (10), 2796−2809.
(45) Otero, E.; Shipman, P. O.; Abd-El-Aziz, A. S.; Urquhart, S. G. Substituent Effects in the Iron 2p and Carbon 1s Edge Near-Edge X-Ray Absorption Fine Structure Spectroscopy of Metal Arene Complexes and Polymers. *Organometallics* **2009**, *28* (7), 2160−2172.
(46) Ruehl, E.; Hitchcock, A. P. Carbon K-Shell Excitation of Metallocenes. *J. Am. Chem. Soc.* **1989**, *111* (14), 5069−5075.
(47) Stevens, P. A.; Madix, R. J.; Stöhr, J. The Bonding of Acetonitrile and $CH_2CN$ on Ag(110) Determined by near Edge X-ray Absorption Fine Structure: Evidence for Π-donor Bonding and Azimuthal Ordering. *J. Chem. Phys.* **1989**, *91* (7), 4338−4345.
(48) Sharnoff, M. Electron Paramagnetic Resonance and the Primarily 3*d* Wavefunctions of the Tetrachlorocuprate Ion. *J. Chem. Phys.* **1965**, *42* (10), 3383−3395.
(49) Gewirth, A. A.; Cohen, S. L.; Schugar, H. J.; Solomon, E. I. Spectroscopic and Theoretical Studies of the Unusual EPR Parameters of Distorted Tetrahedral Cupric Sites: Correlations to x-Ray Spectral Features of Core Levels. *Inorg. Chem.* **1987**, *26* (7), 1133−1146.
(50) Didziulis, S. V.; Cohen, S. L.; Gewirth, A. A.; Solomon, E. I. Variable Photon Energy Photoelectron Spectroscopic Studies of Copper Chlorides: An Experimental Probe of Metal-Ligand Bonding and Changes in Electronic Structure on Ionization. *J. Am. Chem. Soc.* **1988**, *110* (1), 250−268.
(51) Shadle, S. E.; Penner-Hahn, J. E.; Schugar, H. J.; Hedman, B.; Hodgson, K. O.; Solomon, E. I. X-Ray Absorption Spectroscopic Studies of the Blue Copper Site: Metal and Ligand K-Edge Studies to Probe the Origin of the EPR Hyperfine Splitting in Plastocyanin. *J. Am. Chem. Soc.* **1993**, *115* (2), 767−776.


https://doi.org/10.1021/acs.inorgchem.4c01666
*Inorg. Chem.* 2024, 63, 15557−15562

(52) Hedman, B.; Hodgson, K. O.; Solomon, E. I. X-Ray Absorption Edge Spectroscopy of Ligands Bound to Open-Shell Metal Ions: Chlorine K-Edge Studies of Covalency in Tetrachlorocuprate(2-). *J. Am. Chem. Soc.* **1990**, *112* (4), 1643−1645.
(53) Hitchcock, A. P.; Brion, C. E. K-Shell Excitation of HF and $F_2$ Studied by Electron Energy-Loss Spectroscopy. *J. Phys. B At. Mol. Phys.* **1981**, *14* (22), 4399−4413.
(54) Bodeur, S.; Marchal, J. L.; Reynaud, C.; Bazin, D.; Nenner, I. Chlorine K Shell Photoabsorption Spectra of Gas Phase HCI and Cl2Molecules. *Z. Für Phys. At. Mol. Clust.* **1990**, *17*, 291−298.
(55) Filipponi, A. Deconvolution of the Lifetime Broadening from X-Ray Absorption Spectra of Atomic and Molecular Species. *J. Phys. B At. Mol. Opt. Phys.* **2000**, *33* (15), 2835.
(56) Piepho, S. B.; Schatz, P. N. *Group Theory in Spectroscopy*; Wiley: New York, 1983.
(57) Cowan, R. D. *The Theory of Atomic Structure and Spectra*; University of California Press, 1981.
(58) Gusmeroli, R.; Dallera, C. *Missing 1.11*; 2004.
(59) Henke, B. L.; Gullikson, E. M.; Davis, J. C. X-Ray Interactions: Photoabsorption, Scattering, Transmission, and Reflection at E = 50−30000 eV, Z = 1−92. *At. Data Nucl. Data Tables* **1993**, *54* (2), 181−342.


https://doi.org/10.1021/acs.inorgchem.4c01666
*Inorg. Chem.* 2024, 63, 15557−15562